

Linear-response calculation of dynamical spin susceptibility in doped CaCuO_2

V. S. Oudovenko and S. Savrasov

Department of Physics and Astronomy and Center for Condensed Matter Theory, Rutgers University, Piscataway, New Jersey 08854
and Max-Planck-Institut für Festkörperforschung, Heisenbergstrasse 1, D-70569 Stuttgart, Germany

(Received 30 October 2000; published 27 February 2001)

Using the density-functional linear-response theory we calculate momentum and energy dependencies of dynamical spin susceptibility for the optimally doped infinite-layer compound CaCuO_2 . Incommensurate antiferromagnetic fluctuations are obtained in a low-energy region in the normal phase at optimal doping. The results of the calculations are compared with inelastic neutron-scattering measurements and previous model calculations.

DOI: 10.1103/PhysRevB.63.132401

PACS number(s): 75.40.Gb, 71.15.Mb, 75.10.Lp

It is by now widely recognized that studying dynamical spin susceptibility $\chi(\mathbf{q}, \omega)$ of high-temperature superconductors (HTSC) may bring an understanding of their many unusual properties including effect of superconductivity (SC) itself. Among these properties, such issues as opening of the pseudogap, the existence of 41 meV resonance peak in superconducting state and its suppression in the normal state, as well as the incommensurability of magnetic fluctuations and its universality in different HTSC's are most puzzling.¹

Incommensurate spin dynamics has been clearly detected in single-layer La-based cuprates while with bilayer Y-based cuprates the situation is still unclear. Until recent time no clear incommensurability was detected in 123O_{6+x} compounds. Dai *et al.*² have found incommensurate phase in $123\text{O}_{6.6}$ ($T_c = 63$ K) around energy $E = 25$ meV for $T < 70$ K. Later, Mook *et al.*,³ using more advanced experimental technology, succeeded to determine the precise displacements of the incommensurate peaks and found their absolute amplitudes. Recent experiments in $123\text{O}_{6.7}$ revealed an incommensurability at wave vectors $(0.5 \pm \delta, 0.5)$, $(0.5, 0.5 \pm \delta)$, where $\delta \approx 0.11$ which is very close to the hole concentration $\sim \frac{1}{8}$.⁴ Some signs of incommensurability as a flat-topped form of low-energy momentum scans were reported some years ago.^{5,6} It was found⁶ a separable model for the susceptibility, $\chi''(\mathbf{q}, \omega) = \chi''(\omega)F(\mathbf{q})$ where q -dependent shape function, $F(\mathbf{q})$, was the same in both the superconducting and normal states. In other experiments only commensurate magnetic fluctuations were detected.^{7,8} For example, in the work of Bourges⁸ it is reported that momentum dependence of $\chi(q, \omega_0)$ for some fixed ω_0 between 10 and 40 meV and $T = 100$ K shows a commensurate peak at $Q = (\pi, \pi)$ for any doping. In the most recent and a comprehensive inelastic neutron-scattering study of the near optimally doped $\text{YBa}_2\text{Cu}_3\text{O}_{6.85}$ done by Bourges *et al.*⁹ no indication of was found incommensurate magnetic fluctuations above the superconducting temperature.

A great amount of theoretical work has been made to understand the structure of measured $\chi(\mathbf{q}, \omega)$ in both normal and superconducting states. A phenomenological antiferromagnetic Fermi-liquid theory has been developed.¹⁰ Quantum Monte Carlo studies of a two-dimensional (2D) Hubbard model have been carried out.¹¹ In other works,^{12–17} starting from a particular model for the band structure, the calculations of Lindhard and random-phase-approximation like (RPA) susceptibilities have been performed. The calculations

differ by either using a single-band^{12,13,17} or more realistic few-band model^{14–16} and whether the antiferromagnetic (AF) exchange interaction used in the RPA expression is \mathbf{q} dependent.^{13–17} or \mathbf{q} independent.¹²

Both inconsistent experimental situations about the existence of incommensurability in the normal state and numerous model calculations inspired us to perform a realistic simulations of the dynamical spin susceptibility in the normal state by taking into account the effects of *all* bands and by including the effects of *all* local fields. These calculations are based on *ab initio* density-functional linear response approaches and do not use any adjustable parameters. The method has been developed recently¹⁸ and is shown to produce $\chi(\mathbf{q}, \omega)$ in a number of ferromagnetic (Fe, Ni), antiferromagnetic (Cr), and strongly paramagnetic (Pd) metals in good agreement with experiments. The treatment of all bands and all local-field effects is achieved by using linear-muffin-tin-orbital (LMTO) representation¹⁹ when calculating dynamical susceptibilities. The interactions between electrons are generally treated using so-called adiabatic local-density approximation (ALDA).²⁰ The well-known drawback of the latter in case of Cu 3d electrons of HTSC's,²¹ connected with strong underestimation of on-site effective Coulomb interaction, is overcome by using the LDA+*U* density functional.²² The latter substitutes wrong value of Stoner parameter *I* in the LDA functional by the correct value given by the Hubbard *U*. We thus solve self-consistently the following RPA-like equation:

$$\chi_{\mathbf{q}}(\mathbf{r}, \mathbf{r}', \omega) = \chi_{\mathbf{q}}^{(0)}(\mathbf{r}, \mathbf{r}', \omega) + \int \chi_{\mathbf{q}}^{(0)}(\mathbf{r}, \mathbf{r}'', \omega) \times I_{xc}(\mathbf{r}'', \mathbf{r}''') \chi_{\mathbf{q}}(\mathbf{r}''', \mathbf{r}', \omega) d\mathbf{r}'' d\mathbf{r}''' \quad (1)$$

in terms of localized-orbital representation provided by the LMTO. Here, $\chi_{\mathbf{q}}^{(0)}(\mathbf{r}, \mathbf{r}', \omega)$ is noninteracting spin susceptibility and $I_{xc}(\mathbf{r}, \mathbf{r}')$ is assumed to have two energy-independent contributions: the local one [$\sim \delta(\mathbf{r} - \mathbf{r}')$] described by ALDA and the correction for Hubbard *U*, which, however, enters only between the matrix elements of Cu 3d orbitals. This is the only essential approximation made in this calculation. Linear-response functions in Eq. (1) are then represented as one-center spherical harmonics expansions inside the spheres surrounding every atom and as plane-wave expansions in the interstitial region. The well-known problems of the summations over higher excited states and the

matrix inversion are avoided using the solid-state generalization of the Sternheimer method as described in Ref. 18. All calculations are performed for $T=0$.

Since our method does not yet allow us to treat large unit cells and, hence, a well-characterized stoichiometric, nearly optimally doped high-temperature superconductor such as $\text{YBa}_2\text{Cu}_3\text{O}_7$ (YBCO), we consider the compound $(\text{Ca}_{1-x}\text{Sr}_x)_{1-y}\text{CuO}_2$ with $T_c=110$ K (for $x\sim 0.7$ and $y\sim 0.1$)²³ whose simple infinite-layer structure makes it attractive for theoretical studies. We did doping of CaCuO_2 by holes in a uniform neutralizing background charge. The doping was chosen, to what we believe is nearly optimal, equal to 0.24 holes per unit cell and $y=0$. Since the calculated band structure of CaCuO_2 is similar to those found in calculations for $\text{YBa}_2\text{Cu}_3\text{O}_7$, Fermi surfaces (FS) of both cuprates look quite identical and we hope that our results for CaCuO_2 are rather generic for HTSC's near optimal doping. Our earlier studies²⁴ of its lattice dynamics and the strength of the electron-phonon interactions in both s - and d -wave channels confirm this conclusions. Technical details of this calculation are similar to those published earlier.²⁴

We now discuss our results on calculated static spin susceptibility $\chi(\mathbf{q}, \omega=0)$ and the doping dependent value of screened Coulomb interaction U . In the paramagnetic phase of undoped CaCuO_2 , this function exhibits a singularity at wave vector $\mathbf{Q}=(\pi, \pi)$ (and Neel temperature T_N) which signalizes the antiferromagnetic instability in the system. Upon doping, this singularity is smeared out and the system remains paramagnetic at all temperatures while exhibiting strong antiferromagnetic fluctuations. Our $\chi(\mathbf{q})$ calculated at zero doping shows a peak at (π, π) already for $U=0$. However, the peak is found to be too weak to drive the system to antiferromagnetism. This is the well-known drawback of the LDA exchange-correlation interaction.²¹ Upon increasing U , the peak at (π, π) grows up and the system becomes AF instable already at values of U starting from 2.5 eV. In our calculations we used $U=2.1$ eV in order to avoid getting into the insulating regime.

The value of $U=2$ eV for optimally doped HTSC's agrees reasonably well with the data published earlier.^{25,13} By taking into account that the bandwidth of CaCuO_2 , W , which is equal to 3 eV and a small contribution to the total U which comes from the LDA and is of the order 1 eV, the ratio $U_{\text{tot}}/W \approx 1$ is obtained. Our calculations therefore support the regime of intermediate correlations hardly accessible via perturbative treatment.

The calculated dependence of static susceptibility as a function of \mathbf{q} for $U=2$ eV is shown in Fig. 1(a). The effect of the matrix elements resulting in the antiferromagnetically enhanced $\chi(\mathbf{q})$ resolves difficulties of some previous model calculations. It is well known that since Fermi surfaces of LSCO ($\text{La}_{2-x}\text{Sr}_x\text{CuO}_4$) and YBCO compounds are rotated by 45° relative each other, there is in general no problem to explain incommensurate antiferromagnetism of La-based compounds due to Fermi surface nesting, but the same explanation does not work in the YBCO case due to lack of the latter. As a result, in order to recover AF state of YBCO, a strongly \mathbf{q} -dependent exchange interaction $J(\mathbf{q})$ enhanced at (π, π) is standardly placed in the denominator of standard

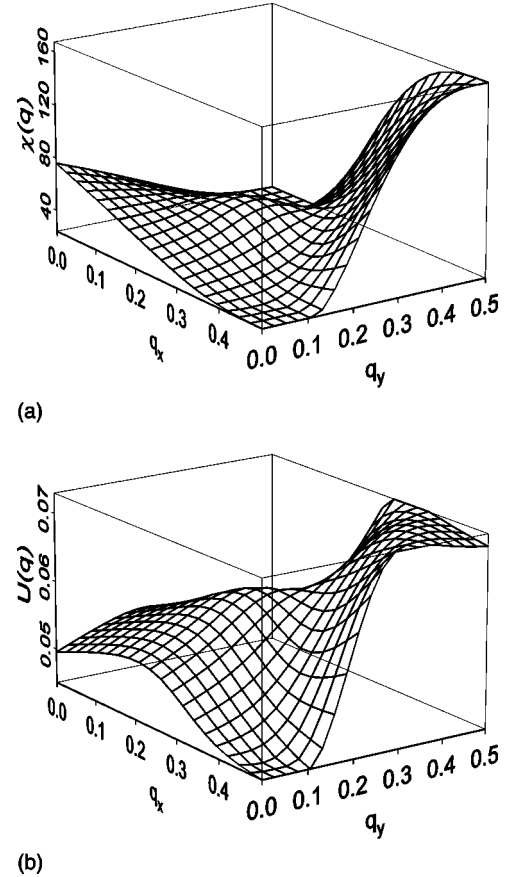


FIG. 1. Static susceptibility $\chi(\mathbf{q})$ (a) and effective momentum dependence of Coulomb interaction $U(\mathbf{q})$ (b) for the doped CaCuO_2 compound. $U(\mathbf{q})$ is given in Rydberg. In our computations the static susceptibility is normalized in such a way that it is equal to the density of states at $q=0$.

random-phase approximation equation for susceptibility.²⁵ Our *ab initio* calculations of doped CaCuO_2 do not make any assumptions of that kind due to the correct inclusion of all band and all matrix element features, while the compound has the Fermi surface geometry very similar to the YBCO. On the other hand, we can also determine an effective \mathbf{q} -dependent interaction $U_{\text{eff}}(\mathbf{q})$ from the relationship $U_{\text{eff}}(\mathbf{q}) = \chi_0^{-1}(\mathbf{q}) - \chi^{-1}(\mathbf{q})$. This will give us correct downfolding of our full multiband calculation to the one-band model. The behavior of function $U_{\text{eff}}(\mathbf{q})$ is shown in Fig. 1(c) which actually shows the enhancement around the vector (π, π) .

Assuming nearest- and next-nearest-neighbor interactions, we have fitted the function $U_{\text{eff}}(\mathbf{q})$ to $U_0 + U_{nn}[\cos(q_x a) + \cos(q_y a)] + 2U_{nnn}[\cos(q_x a)\cos(q_y a)]$. The extracted values of U_0 , U_{nn} , and U_{nnn} are equal to 0.74, -0.07, and 0.06 eV, correspondingly. This result allows us to conclude that the model with nearest-neighbor interactions used earlier²⁵ may not be completely adequate for the HTSC's and the inclusion of next interactions is seen to be equally important.

We now turn our discussion to the incommensurability issue. As already seen from Fig. 1(a) there exists a whole plateau around the point (π, π) which assumes no clear commensurate structure. The incommensurability becomes

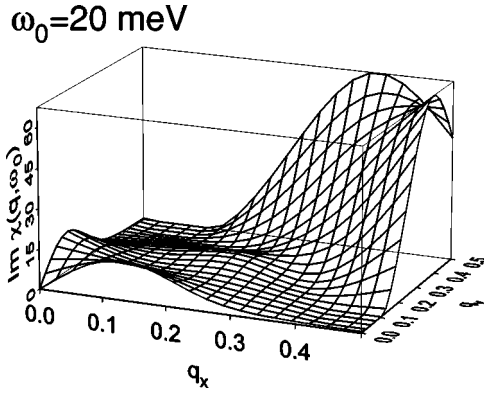


FIG. 2. Momentum dependence of an imaginary part of dynamical spin susceptibility $\chi(q, \omega)$ for optimally doped CaCuO_2 .

much more pronounced with increasing the frequency. Momentum dependence of $\text{Im}\chi(q, \omega_0)$ at $\omega_0 = 20$ meV is shown in Fig. 2 which undoubtedly demonstrates the existence of incommensurate peaks located at the edges of the BZ. The crucial role in emerging those is played by the Lindhard function which is directly related to the band-structure. This conclusion is in general agreement with our own and previous model calculations.¹⁶

Earlier experiments show only commensurate fluctuations for the YBCO FS geometry.⁷ However, some signs of incommensurability in the flat-topped form have been published.^{5,6} Dai *et al.*² have very recently reported the presence of the incommensurability in YBCO. While their peaks are rotated by 45° relative to our findings, the authors also stressed that the peak structure like ours may also explain the obtained experimental result.

We scanned for incommensurability features in a quite broad frequency region and found that incommensurate picture is very robust at low frequencies (up to 60 meV) and $\text{Im}\chi(q, \omega)$ becomes almost featureless for higher energies. It comes from our calculations that incommensurability vector is almost frequency independent at low energies.

We checked $\text{Im}\chi(q, \omega)$ for incommensurability at another doping and found no incommensurate fluctuations in the overdoped regime at $\delta = 0.18$. The reason for this is the behavior of FS which changes quite substantially with doping. The Fermi surface changes from the rounded one (in underdoped and optimally doped case) to nearly nested one (in overdoped case). As a result, the static susceptibility changes dramatically and has monotonous behavior with no signs of incommensurability at all.

Thus, we have obtained incommensurate magnetic fluctuations in doped CaCuO_2 compound in the normal state without taking into account superconducting *s*- or *d*-wave picture proposed in a number of theoretical works^{26,27} to explain this phenomenon. In our case incommensurability comes from band-structure singularities where combination of “itinerant” and “localized” contributions are taken into account.¹³

We finally discuss frequency dependence of the dynamical spin susceptibility. Calculated $\text{Im}\chi(\mathbf{q}, \omega)$ of optimally doped CaCuO_2 for $\mathbf{q} = (\pi, \pi)$ is presented in Fig. 3, where our results are compared with the results of neutron-

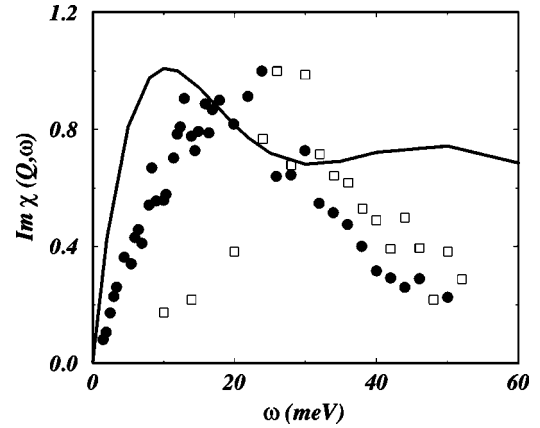


FIG. 3. Frequency dependence of $\text{Im}\chi(Q, \omega)$ of optimally doped CaCuO_2 (solid line) and experimental data for $\text{YBa}_2\text{Cu}_3\text{O}_{6.5}$ (filled circles) and $\text{YBa}_2\text{Cu}_3\text{O}_{6.92}$ (squares).

scattering measurements for $123\text{O}_{6.5}$ ($T_c = 53$ K) and $123\text{O}_{6.92}$ ($T_c = 91$ K).⁸ All curves have been normalized to unity. Our calculation clearly shows a peak at $\omega = 10$ meV originating from spin fluctuation at (π, π) . This peak is present for all \mathbf{q} 's near (π, π) but rapidly disappears when \mathbf{q} goes inside the Brillouin zone. As we see, the calculated curve is in a reasonable agreement with the experiment. In fact, a better agreement is found with the underdoped YBCO sample ($\text{O}_{6.5}$, $T_c = 53$ K) whose peak position is at $\omega = 25$ meV. However, due to some differences in the band structures of YBCO and CaCuO_2 which can lead to slightly different determination of optimal doping, the discrepancies of such kind are expectable. To illustrate doping dependence of the peak position, we have computed $\text{Im}\chi(\mathbf{q}, \omega)$ for $\delta = 0.18$ which corresponds to 0.36 holes per unit cell. The peak has been found to shift from $\omega \approx 10$ meV to $\omega \approx 20$ meV in accord with the experimental trends.

Another feature of our calculation is an existence of some plateau at frequencies of the order 50 meV which is not seen in the YBCO experiments. It originates from the π band lying very close to the Fermi level in doped CaCuO_2 . This band is specific for this system only and is not found in YBCO and other HTSC's. The latter gives possible explanation for our discrepancy in this region.

In conclusion, we have calculated momentum and energy dependencies of real and imaginary parts of the dynamical spin susceptibility $\chi(\mathbf{q}, \omega)$ of doped CaCuO_2 compound using *ab initio* density-functional linear-response approach. Our fermiological description of incommensurate magnetic fluctuations is found to be in good agreement with the existing neutron-scattering measurements and previous model calculations. We therefore believe that our picture is adequate for this system and, most likely, for other HTSC's in the normal state at optimal doping. Extensions of the present calculation to the superconducting state and to the finite temperatures are possible and will be postponed for the future work.

The authors thank O. K. Andersen, A. Liechtenstein, B. Keimer, and G. Khaliullin for many helpful discussions.

- ¹M. Imada, A. Fujimori, and Y. Tokura, *Rev. Mod. Phys.* **70**, 1039 (1998).
- ²P. Dai, H. Mook, and F. Doğan, *Phys. Rev. Lett.* **80**, 1738 (1998).
- ³H.A. Mook, P. Dai, S.M. Hayden, G. Aeppli, T.G. Perring, and F. Doğan, *Nature (London)* **395**, 580 (1998).
- ⁴M. Arai, T. Nishijima, Y. Endoh, T. Egami, S. Tajima, K. Tomimoto, Y. Shiohara, M. Takahashi, A. Garrett, and S.M. Bennington, *Phys. Rev. Lett.* **83**, 608 (1999).
- ⁵J. Tranquada, P. Gehring, and G. Shirane, *Phys. Rev. B* **46**, 5561 (1992).
- ⁶B. Sternlieb, J. Tranquada, and G. Shirane, *Phys. Rev. B* **50**, 12 915 (1994).
- ⁷J. Rossat-Mignot *et al.*, in *Selected Topics in Superconductivity*, edited by L. Gupta and M. Multani (World Scientific, Singapore, 1993), Vol. 1, p. 265.
- ⁸P. Bourges, in *The Gap Symmetry and Fluctuations in High Temperature Superconductors*, edited by J. Bok, G. Deutscher, D. Pavuna and S. A. Wolf (Plenum Press, 1998); P. Bourges, cond-mat/9901333 (unpublished).
- ⁹P. Bourges, Y. Sidis, H.F. Fong, L.P. Regnault, J. Bossy, A. Ivanov, and B. Keimer, *Science* **288**, 1234 (2000).
- ¹⁰A.J. Millis, H. Monien, and D. Pines, *Phys. Rev. B* **42**, 167 (1990).
- ¹¹N. Furukawa and M. Imada, *J. Phys. Soc. Jpn.* **61**, 3331 (1992).
- ¹²N. Bulut and D. Scalapino, *Phys. Rev. B* **47**, 3419 (1993); **53**, 5149 (1996).
- ¹³F. Onufrieva and J. Rossat-Mignot, *Phys. Rev. B* **52**, 7572 (1995).
- ¹⁴D. Liu, Y. Zha, and K. Levin, *Phys. Rev. Lett.* **75**, 4130 (1995).
- ¹⁵Y. Zha, K. Levin, and Q. Si, *Phys. Rev. B* **47**, 9124 (1993).
- ¹⁶Q. Si, Y. Zha, and K. Levin, *Phys. Rev. B* **47**, 9055 (1993).
- ¹⁷T. Tanamoto, H. Kohno, and H. Fukuyama, *J. Phys. Soc. Jpn.* **62**, 717 (1993); **62**, 1455 (1993).
- ¹⁸S. Savrasov, *Phys. Rev. Lett.* **81**, 2570 (1998).
- ¹⁹O. Andersen, *Phys. Rev. B* **12**, 3060 (1975).
- ²⁰E. Runge and E.K.U. Gross, *Phys. Rev. Lett.* **52**, 997 (1984); E.K.U. Gross and W. Kohn, *ibid.* **55**, 2850 (1984).
- ²¹See, for e.g., W.E. Pickett, *Rev. Mod. Phys.* **61**, 433 (1989).
- ²²V.I. Anisimov, J. Zaanen, and O.K. Andersen, *Phys. Rev. B* **44**, 943 (1991).
- ²³M. Azuma *et al.*, *Nature (London)* **356**, 775 (1992).
- ²⁴S.Y. Savrasov and O.K. Andersen, *Phys. Rev. Lett.* **77**, 4430 (1996).
- ²⁵K. Levin, Ju H. Kim, J.P. Lu, and Q. Si, *Physica C* **175**, 449 (1991).
- ²⁶M. Lavagna and G. Stemann, *Phys. Rev. B* **49**, 4235 (1994).
- ²⁷H. Kee and Y.B. Kim, *Phys. Rev. B* **59**, 4470 (1999); J.P. Lu, *Phys. Rev. Lett.* **68**, 125 (1992).